J. Phys.: Condens. Matter **22** (2010) 065404 (5pp) doi:10.1088/0953-8984/22/6/065404

The strength of single crystal copper under uniaxial shock compression at 100 GPa

W J Murphy[1], A Higginbotham[1], G Kimminau[1], B Barbrel[2], E M Bringa[3], J Hawreliak[4], R Kodama[5], M Koenig[2], W McBarron[6], M A Meyers[7], B Nagler[1], N Ozaki[5], N Park[6], B Remington[4], S Rothman[6], S M Vinko[1], T Whitcher[1] and J S Wark[1]

[1] Department of Physics, Clarendon Laboratory, University of Oxford, Parks Road, Oxford OX1 3PU, UK
[2] Laboratoire pour l'Utilisation des Lasers Intenses, UMR7605, CNRS-CEA-Université Paris VI-École Polytechnique, 91128 Palaiseau, France
[3] Instituto de Ciencias Basicas, Universidad Nacional de Cuyo, Mendoza, Argentina
[4] Lawrence Livermore National Laboratory, Livermore, CA 94550, USA
[5] Graduate School of Engineering, Osaka University, Suita, Osaka 565-0871, Japan
[6] Material Modelling Group, AWE, Aldermaston, Reading, Berkshire RG7 4PR, UK
[7] Materials Science and Engineering Program, University of California, San Diego, CA 92093, USA

E-mail: justin.wark@physics.ox.ac.uk

Received 20 September 2009, in final form 14 December 2009
Published 22 January 2010
Online at stacks.iop.org/JPhysCM/22/065404

Abstract

In situ x-ray diffraction has been used to measure the shear strain (and thus strength) of single crystal copper shocked to 100 GPa pressures at strain rates over two orders of magnitude higher than those achieved previously. For shocks in the [001] direction there is a significant associated shear strain, while shocks in the [111] direction give negligible shear strain. We infer, using molecular dynamics simulations and VISAR (standing for 'velocity interferometer system for any reflector') measurements, that the strength of the material increases dramatically (to ∼1 GPa) for these extreme strain rates.

1. Introduction

Despite many decades of study, the response of materials under shock compression at ultra-high strain rates (10^6–10^{10} s^{-1}) remains poorly understood. In particular, whilst it is known that for many materials the supportable shear stress increases with plastic strain rate, $\dot{\epsilon}_p$, such measurements have largely been limited to relatively modest values of $\dot{\epsilon}_p$. For example, in the case of copper, Follansbee and Gray used a Kolsy–Hopkinson bar technique to measure shear stress at $\dot{\epsilon}_p$ between 10^{-4} and 10^4 s^{-1} [1], whilst Tong and co-workers extended the range to above 10^6 s^{-1} by use of a pressure–shear technique [2] and Meyers and co-workers reached rates of 10^7 s^{-1} using laser-induced shocks [3]. The results of these studies are shown in figure 1. However, above these strain rates direct measurements of metallic strength have hitherto been inaccessible. The issue has not been an inability to subject materials to such high values of $\dot{\epsilon}_p$. In their classic paper Swegle and Grady note that within a steady shock, $\dot{\epsilon}_p$ for a large range of materials scales as the fourth power of the peak applied stress [4]. An extrapolation of their results for copper at low strain rates ($<10^7$ s^{-1}) indicates that $\dot{\epsilon}_p$ of order 10^{10} s^{-1} will be achieved for shock pressures below 100 GPa—a pressure region which can readily be accessed. The difficulty in experimentally assessing material strength at high $\dot{\epsilon}_p$ and high pressures has been the lack of direct experimental techniques for making such measurements (although some data has been obtained in shock-release measurements) [5, 6]. Furthermore, VISAR [7] measurements at quite high pressures, via ramped compression, indicate that the yield stress of aluminium may rise to around several GPa for shocks up to 70 GPa, but the error bars in this regime are extremely large [8]. From the theoretical standpoint, non-equilibrium molecular dynamics (NEMD) calculations of the shear strength of copper at ultra-high strain rates, in excess of 10^9 s^{-1}, indicate that a shear

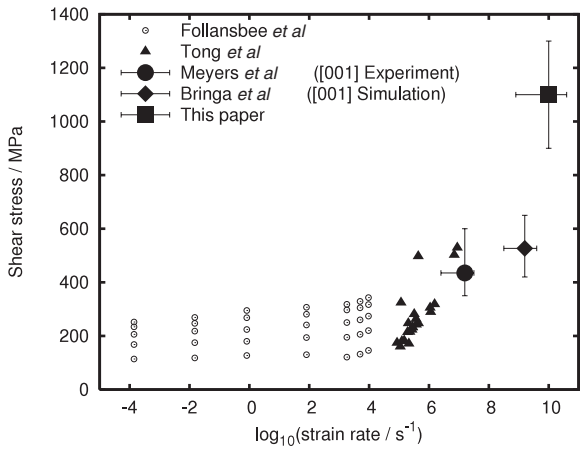

Figure 1. Shear stress of copper at various strain rates. Data taken from experiments [3, 2, 26] and current estimates, and from molecular dynamics simulations [9].

stress approaching 1 GPa can be supported [9]. Importantly, these NEMD simulations are consistent with an extrapolation of the lower strain rate data, and an experimental verification of these results would provide an important demonstration of the validity of the scaling between material strength and strain rate over 6 orders of magnitude.

Time resolved x-ray diffraction from shocked materials is a technique that has emerged over recent years as a useful tool in shock physics [10–14]. Importantly, it affords the possibility of providing direct information about material strength, but by measuring elastic *strains*, rather than stresses. Some types of defects may also shift the position of the Bragg peaks, but despite the relatively high defect densities anticipated, this correction is expected to be minor [15, 16]. Thus, invoking the normal assumptions of stresses supported by elastic strains, and zero plastic dilatation, simultaneous measurements of the lattice parameters in directions perpendicular and parallel to the shock propagation direction will provide a direct measure of volumetric compression and shear strain.

To date, all measurements using *in situ* diffraction to study shock-compressed matter have been limited to shock pressures of order 32 GPa or less [17]. An extension of this pressure range to the 100 GPa regime would not only open up the range of strain rates that can be studied in shocked materials, as noted above, but also demonstrate the viability of the x-ray technique for obtaining information about the crystal lattice under transient shock conditions at pressures rivalling those that can be achieved in diamond anvil cells.

In this paper we report the first direct measurements of shear strain in single crystal copper at shock pressures in excess of 100 GPa. We demonstrate a shear strength at these ultra-high strain rates (of order 10^{10} s^{-1}) which is both broadly in agreement with the extrapolation of the lower strain rate data and with non-equilibrium molecular dynamics simulations, and note that for single crystal copper the observation of shear strain is more readily achieved for shocks propagating along [001], rather than [111], owing to the much smaller shear modulus in this direction.

2. Experimental details

The experiments were performed in Target Area East of the VULCAN high-power laser system [18] at the Rutherford Appleton Laboratory in the UK. Samples of 10 μm thick, single crystal copper, 5 mm in diameter, were coated with 19.5 μm of Parylene-N and then 0.3 μm of aluminium. These samples were shock loaded by direct laser radiation of the Al-coated side of the target with 1.053 μm laser radiation in a laser spot of diameter approximately 2 mm. These pulses had a rise time of 150 ps to a maximum value, after which there was a fall off to around half that value over 6 ns, followed by a linear fall within 200 ps. The energy in the laser beams could be varied up to a total 1250 J, providing an average irradiance of up to almost 10^{13} W cm^{-2}.

The velocity of the rear surface (i.e. opposite to the irradiated surface) was measured along the shock propagation direction of the single crystal by use of a twin bed line VISAR system. The VISAR signals were recorded on streak cameras with a sweep speed of 1 ns mm^{-1}, which gave a time window of order 20–25 ns. On one bed a 28.8 mm etalon was used giving a velocity per fringe of 1.729 km s^{-1} with temporal resolution of 150 ps and on the second bed a 50 mm etalon was used resulting in a velocity per fringe of 0.996 km s^{-1} with a temporal resolution of 260 ps.

Simultaneously with the VISAR measurements, the state of strain within the shocked crystals was monitored by *in situ* divergent beam x-ray diffraction [19]. Quasi-monochromatic iron He-α x-rays were created by illuminating an iron foil located 1 mm from the crystal surface with a 1 ns, 150 J pulse of 527 nm wavelength laser radiation, focused to a 25 μm spot. X-rays diverging from this point source irradiated the crystal at a range of angles, being diffracted when they matched the appropriate Bragg condition, and recorded on large area image plate detectors placed several cm from the x-ray source and crystal. The beams were timed such that the backlighter beams struck the foil $\sim$2.5 ns after the drive beam hit the target. The crystals were sufficiently thin to allow the diffraction patterns to be recorded simultaneously in both reflected and transmitted geometries. The x-ray source was positioned to within $\pm$20 μm of a reference point on the crystal. Fitting the positions of the detectors relative to the crystal to multiple lines from the unshocked crystal means that the dominating source of error is the original crystal quality and the finite bandwidth of the x-ray source. The errors in strain were estimated from the variation in the shift of the intensity peak of the diffraction line from the shocked region.

Furthermore, this alignment procedure allowed us to determine the position on the surface of the crystal from which x-rays were being diffracted, with respect to the centre of the shock-drive laser beams, to an accuracy of $\pm$50 μm. The VISAR traces showed that the shock breakout occurs within a 150 ps window over a 1.2 mm region of the crystal, and the position of the x-ray source was set to ensure that the diffracted x-rays used for determining the degree of longitudinal and transverse strain within the shock were scattered from this region of the crystal. As well as the VISAR, the large angle x-ray detectors allowed us to determine that the shock was

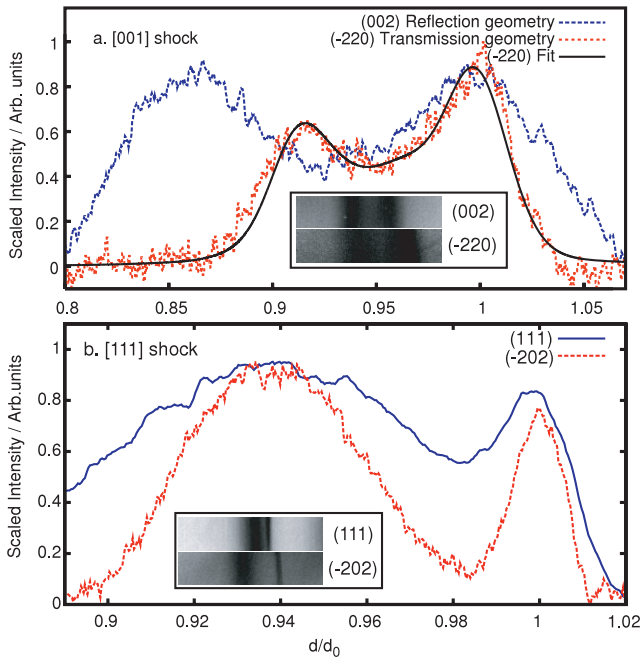

Figure 2. The intensity profiles for the shocked and unshocked peaks measured in reflection geometry and in transmission geometry and the strain deduced for (a) [001] shock, where (002) was the reflected peak and $(\bar{2}20)$ was the transmitted peak, and (b) [111] shock where (111) was the reflected peak and $(\bar{2}20)$ was the transmitted peak. (a) Also shows the predicted intensity profile calculated for a 10 μm copper crystal compressed to 9% transverse strain over 2.5 μm, where the dislocation density in the shocked region is 2.5×10^{13} cm^{-2}. Insets show raw data from which the lineouts were taken. d denotes the interplanar spacing with d_0 giving the interplanar spacing at room temperature and pressure.

(This figure is in colour only in the electronic version)

spatially uniform on mm length scales by measuring strain as a function of position across the surface of the crystal. We find the compression of the lattice (both parallel and perpendicular to the shock direction) to be uniform within 0.5% on a mm scale length: thus we know that the shock is uniaxial in nature.

3. Experimental results

For shocks along the [001] direction the compression in the shock direction was measured from the (002) Bragg peak, whilst on the same shot the strain perpendicular to the shock direction was measured from the $(\bar{2}20)$ peak. The image plate data is shown in figure 2, along with a plot of diffracted intensity against strain for each of the relevant directions. We observe a compression along the shock direction of $13 \pm 1\%$, and $9 \pm 1\%$ perpendicular to the shock direction—giving a value of V/V_0 of 72%. This corresponds to a shear strain of 0.045 where the shear strain is given by

$$\gamma = \tan\alpha = \tan\left[2\tan^{-1}\left(\frac{1-\epsilon_{x/y}}{1-\epsilon_z}\right) - \frac{\pi}{2}\right], \qquad (1)$$

where ϵ_z is the compressive strain in the direction in which the shock is travelling and $\epsilon_{x/y}$ is the transverse compressive strain. α is the change in the angle between the two perpendicular material line elements in the undeformed material, where the line elements are chosen to maximize α.

Table 1. Summary of atomic strains and particle velocities measured and shock pressures inferred from the SESAME equation of state [22]. U_p is the shock particle velocity.

Shock direct.	Long. strain (%)	Trans. strain (%)	Total comp. (%)	U_p (km s^{-1})	Pressure (GPa)
[001]	13 ± 1	9 ± 1	28 ± 2	1.85 ± 0.05	112 ± 5
[111]	6 ± 1	6 ± 1	17 ± 3	1.0 ± 0.05	50 ± 4
[111]	5 ± 1	5 ± 1	14 ± 3	0.6 ± 0.05	26 ± 4

For shocks along the [111] direction the compression in the shock direction was measured from the (111) peak whilst on the same shot the strain perpendicular to the shock direction was measured from the $(\bar{2}02)$ peak. In this case it is found that there is no measurable difference between the lattice strains parallel to the shock direction and strains perpendicular to the shock direction up to pressures of 50 GPa, a point to which we shall return later. A summary of the experimental data can be found in table 1.

We note that the width of the diffraction signals from the shock-compressed material around the peak value is considerable. If the scattering of x-rays to such high angles were due to much larger compressions than the mean, then it would imply a V/V_0 value of around 0.6. Such a compression requires a pressure of order 400 GPa, totally inconsistent with the VISAR measurements and known pressures for such laser intensities [20], and well above the shock-induced melting pressure [23]. The width of the diffraction from the shocked material is, however, consistent with defect densities of $(2.3 \pm 0.4) \times 10^{13}$ cm^{-2}, which broaden the peak [15]. Such a shock-induced defect density at this pressure agrees well with molecular dynamics simulations by Holian and co-workers [21].

Alongside the experimental data we show the diffraction profile simulated by dynamical diffraction theory [27] assuming an unshocked crystal with a transverse compression increasing to 9% linearly over 2.5 μm, and where the shocked portion is assumed to have a defect density of 2.5×10^{13} cm^{-2}. The region where the compression is increasing linearly is centred on 3 μm from the driven surface. This indicates that the strain rate of the shock was of order 10^{10} s^{-1}. The effect of defects was modelled within the dynamical diffraction framework by randomizing the phase of the diffracted and transmitted fields. This gives diffracted intensity profiles consistent with the theoretical predictions given by the Scherrer equation for crystallite size broadening [15].

The simultaneously measured VISAR signals allow the compression data deduced from x-ray diffraction to be compared with EOS predictions. Taking the particle velocity just before release to be half the free-surface velocity measured with VISAR, we show in figure 3 the experimental diffraction and VISAR data alongside predictions from both the SESAME EOS [22], and the compression particle velocity (U_p) curve deduced by Bringa and co-workers using molecular dynamics to simulate shock waves in copper [23], with the material response modelled using Mishin's embedded atom model (EAM) potential [25]. Excellent agreement is found.

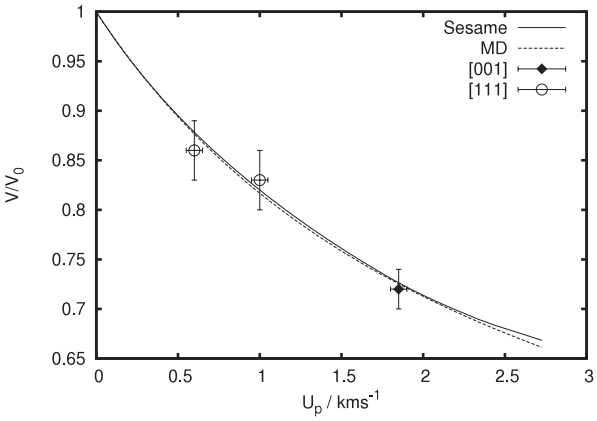

Figure 3. The comparison of shocks along [111] (circles) and [001] (diamonds) with SESAME equation of state predictions and molecular dynamics simulations [23]. The experimental results from VISAR gave the particle velocity and the diffraction data gave the compressions. U_p is the shock particle velocity.

4. MD simulations

For an ideal [001] shock on a perfect crystal with a particle velocity corresponding to our experimental data MD simulations would predict no plasticity, as the shock front would be sufficiently steep to take the crystal directly over the Bain path [28]. In an attempt to model experimental conditions using the molecular dynamics package LAMMPS [24] and Mishin's embedded atom model (EAM) potential, a simulation of a $275 \times 275 \times 7246$ Å sample of copper was set up with voids of radius 25 Å at intervals of 500 unit cells in the [001] shock direction. These voids lower the threshold for nucleation [9]. This size of void was chosen to be below but close to the peak shear stress for uniaxial compression along the Bain path (peak at ∼3 GPa) in order to force dislocations before that peak, whilst also not having the activation stress so low that its effects would dominate the residual shear stress. This was then thermalized for 2 ps to 300 K. Atoms within two conventional cells of $z = 0$ were fixed and accelerated linearly in the positive z direction to a maximum speed of 1.85 km s^{-1} over 30 ps. The resulting strains in the ramped section long after the ramp had passed were $\epsilon_z = 14 \pm 0.5\%$ and $\epsilon_{x/y} = 8.5 \pm 0.5\%$ with a relaxation timescale of 20 ps. These values are consistent with the experimental values. From this, we infer a shear stress of 1.1 GPa where the shear stress is given by

$$\tau = \tfrac{1}{2}\left[\sigma_{zz} - \tfrac{1}{2}(\sigma_{xx} + \sigma_{yy})\right], \qquad (2)$$

where σ_{ii} is the stress along the axis i, and z is the shock axis. This shear stress corresponding to our experimental data is plotted alongside the lower strain rate data from [3, 2, 26] in figure 1. In the same figure we show the shear stress deduced from MDCASK simulations performed by Bringa and co-workers [9]. Despite good agreement between the MD and experimental data, as a caveat we note that the experiments were performed on timescales at least one order of magnitude longer than can yet be accessed by MD simulations. We note that the differences in shear stress for low strain rates are due to differences in the final strain values [26]. There are insufficient data at higher strain rates to quantify the effect of strain on shear stress supported.

As noted above, and as seen in figure 2, within the margins of experimental error there is no evidence for a sustained shear strain for those crystals shocked along [111] directions. However, it is important to note that this does not imply that the shear stress is small. High shear stresses along [111] correspond to quite small shear strains, that is, the crystal in the [111] direction is much stiffer than in the [001] direction. This large difference in behaviour is related to the fact that uniaxial compression of an fcc crystal along [001] takes the crystal along the Bain path which has the effect of keeping the shear stress relatively low. Compressing along the [111] direction has no such moderating influence. To examine this effect further we used LAMMPS to investigate shock compression along [111] in Cu. A $616 \times 1067 \times 4715$ Å single crystal of copper having the [111] direction oriented along z was first thermalized to 300 K. To generate the shock all atoms within two conventional cells of $z = 0$ were fixed and then driven as a unit into the crystal in the positive z direction at a particle velocity of 1 km s^{-1}. An x-ray diffraction pattern was simulated by taking the Fourier transform of the coordinates of the relaxed region behind the shock [29]. The elastic strains deduced from the simulated diffraction indicated a shear strain of 0.006 ± 0.002, even though LAMMPS gave a shear stress of around 700 MPa—consistent with a larger shear modulus along this direction. This would indicate that the diffraction technique will work best for samples with small shear moduli. As well as this the mechanism for relieving shear strain may be different for shocks in the [111] and [001] directions [30]. This could influence the final shear strain via the relative ease of dislocation motion through a perfect crystal and also the tendency for dislocations to be pinned by other defects. As well as this the Schmid factors for the $\langle 11\bar{2}\rangle\{111\}$ slip systems are quite different for strains generated by [001] and by [111] shocks.

5. Summary

In summary we have used *in situ* x-ray diffraction to measure shear strains in single crystals of copper shocked to pressures in excess of 100 GPa—a pressure that starts to rival those obtainable in diamond anvil cell experiments. Simultaneous VISAR measurements allow us to show that the compressions deduced from the diffraction data are in agreement with MD and SESAME tables. We find that a shear stress of order 1 GPa is supported for shocks along the [001] direction, at a strain rate of order 10^{10} s^{-1}, a figure which is significantly higher than lower strain rate data, but which follows the trend. Although MD simulations indicate that similarly large shear stresses can be supported along [111], the large shear modulus enables the shear stress to be supported by a much smaller shear strain, which is consistent with our empirical results.

Acknowledgments

The authors gratefully acknowledge financial support from a number of organizations. WJM was supported by AWE

Aldermaston. AH was supported by Daresbury Laboratory through the NorthWest Science Fund. GK has partial support from LLNL under subcontract No. B566832. BN acknowledges support from the EU RTN FLASH. NO was supported by the Core-to-Core Programme from JSPS and the Global COE Programme from MEXT. Resources for large scale computing were provided under the Institutional Grand Computing Challenge at LLNL. The authors thank the target area and laser staff of the VULCAN laser for their help in performing the experiment, and Ray Smith for helpful discussions concerning VISAR.

References

[1] Follansbee P S and Gray G T III 1991 *Mater. Sci. Eng.* A **138** 23
[2] Tong W, Clifton R J and Huang S 1992 *J. Mech. Phys. Solids* **40** 1251
[3] Meyers M A *et al* 2003 *Acta Mater.* **51** 1211
[4] Swegle J W and Grady D E 1985 *J. Appl. Phys.* **58** 692
[5] Vogler T J and Chhabildas L C 2006 *Int. J. Impact Eng.* **33** 812
[6] Luo S N *et al* 2004 *High Press. Res.* **24** 409
[7] Barker L M and Hollenbach R E 1972 *J. Appl. Phys.* **43** 4669
[8] Smith R F *et al* 2007 *Phys. Rev. Lett.* **98** 065701
[9] Bringa E M *et al* 2006 *Nat. Mater.* **5** 805
[10] Johnson Q, Mitchell A and Evans L 1971 *Nature* **231** 310
[11] Rigg P A and Gupta Y M 1998 *Appl. Phys. Lett.* **73** 1655
[12] Kalantar D H *et al* 2005 *Phys. Rev. Lett.* **95** 075502
[13] Loveridge-Smith A *et al* 2001 *Phys. Rev. Lett.* **86** 2349
[14] Whitlock R R and Wark J S 1995 *Phys. Rev.* B **52** 8
[15] Warren B E 1990 *X-Ray Diffraction* (New York: Dover)
[16] Rosolankova K *et al* 2006 *J. Phys.: Condens. Matter* **18** 6749
[17] Kalantar D H *et al* 2000 *Phys. Plasmas* **7** 1999
[18] Danson C N *et al* 1993 *Opt. Commun.* **103** 392
[19] Kalantar D H *et al* 2003 *Rev. Sci. Instrum.* **74** 1929
[20] Benuzzi A *et al* 1996 *Phys. Rev.* E **54** 2162
[21] Holian B L and Lomdahl P 1998 *Science* **280** 2085
[22] Holian K S 1992 *SESAME #3332 Los Alamos National Laboratory Report* No. LA-UR-92-3407
[23] Bringa E M *et al* 2004 *J. Appl. Phys.* **96** 3793
[24] Plimpton S 1995 *J. Comput. Phys.* **117** 1
[25] Mishin Y *et al* 2001 *Phys. Rev.* B **63** 224106
[26] Follansbee P S, Kocks U F and Regazzoni G 1985 *J. Phys. Colloq.* **46** 25
[27] Wie C R, Tombrello T A and Vreeland J T 1986 *J. Appl. Phys.* **59** 3743
[28] Bain E and Dunkirk N 1924 *Trans. AIME* **70** 25
[29] Kimminau G *et al* 2008 *J. Phys.: Condens. Matter* **20** 505203
[30] Germann T C *et al* 2004 *Metall. Mater. Trans.* A **35** 2609